Tumor Dosimetry and Response for [153]Sm-Ethylenediamine Tetramethylene Phosphonic Acid Therapy of High-Risk Osteosarcoma

Srinivasan Senthamizhchelvan[1], Robert F. Hobbs[1,2], Hong Song[1], Eric C. Frey[1], Zhe Zhang[3], Elwood Armour[2], Richard L. Wahl[1,4], David M. Loeb[5], and George Sgouros[1]

[1]Division of Nuclear Medicine, Russell H. Morgan Department of Radiology and Radiological Science, Johns Hopkins University, Baltimore, Maryland; [2]Department of Radiation Oncology and Molecular Radiation Sciences, Johns Hopkins University, Baltimore, Maryland; [3]Division of Biostatistics and Bioinformatics, Sidney Kimmel Comprehensive Cancer Center, Johns Hopkins University, Baltimore, Maryland; [4]Department of Oncology, Johns Hopkins University, Baltimore, Maryland; and [5]Division of Pediatric Oncology, Sidney Kimmel Comprehensive Cancer Center, Johns Hopkins University, Baltimore, Maryland

[153]Sm-ethylenediamine tetramethylene phosphonic acid ([153]Sm-EDTMP) therapy for osteosarcoma is being investigated. In this study, we analyzed the influence of [153]Sm-EDTMP administered activity (AA), osteosarcoma tumor density, mass, and the shape of the tumor on absorbed dose (AD). We also studied the biologic implication of the nonuniform tumor AD distribution using radiobiologic modeling and examined the relationship between tumor AD and response. **Methods:** Nineteen tumors in 6 patients with recurrent, refractory osteosarcoma enrolled in a phase I or II clinical trial of [153]Sm-EDTMP were analyzed using the 3-dimensional radiobiologic dosimetry (3D-RD) software package. Patients received a low dose of [153]Sm-EDTMP (37.0–51.8 MBq/kg), followed on hematologic recovery by a second, high dose (222 MBq/kg). Treatment response was evaluated using either CT or MRI after each therapy. SPECT/CT of the tumor regions were obtained at 4 and 48 h or 72 h after [153]Sm-EDTMP therapy for 3D-RD analysis. Mean tumor AD was also calculated using the OLINDA/EXM unit-density sphere model and was compared with the 3D-RD estimates. **Results:** On average, a 5-fold increase in the AA led to a 4-fold increase in the mean tumor AD over the high- versus low-dose–treated patients. The range of mean tumor AD and equivalent uniform dose (EUD) for low-dose therapy were 1.48–14.6 and 0.98–3.90 Gy, respectively. Corresponding values for high-dose therapy were 2.93–59.3 and 1.89–12.3 Gy, respectively. Mean tumor AD estimates obtained from OLINDA/EXM were within 5% of the mean AD values obtained using 3D-RD. On an individual tumor basis, both mean AD and EUD were positively related to percentage tumor volume reduction ($P = 0.031$ and 0.023, respectively). **Conclusion:** The variations in tumor density, mass, and shape seen in these tumors did not affect the mean tumor AD estimation significantly. The tumor EUD was approximately 2- and 3-fold lower than the mean AD for low- and high-dose therapy, respectively. A dose–response relationship was observed for transient tumor volume shrinkage.

Effective treatment of recurrent, refractory, or metastatic osteosarcoma remains a challenge in oncology. Most often, surgical and external-beam radiotherapy (XRT) strategies target the primary tumor rather than metastases and have a limited efficacy in the treatment of metastatic disease (*1*). Radiopharmaceutical therapy (RPT) is one of the few viable alternatives to chemotherapy for treating patients with recurrent, refractory, or metastatic cancer. [153]Sm-ethylenediamine tetramethylene phosphonic acid ([153]Sm-EDTMP) is being investigated as an RPT agent for osteogenic sarcoma tumors showing ^{99m}Tc-methylene diphosphonate avidity (osteoblastic uptake) (*2–5*). The radionuclide [153]Sm has a physical half-life of 46.5 h and decays by β-particle (maximum energy = 0.81 MeV) emission; photon emissions include a 103-keV photon appropriate for scintigraphic imaging, thereby allowing target localization and image-based dosimetry.

Clinical studies have shown that [153]Sm-EDTMP has therapeutic activity in patients with painful metastatic osteosarcoma or in cases of recurrent bone sites inaccessible to local therapies (surgery, XRT) (*6–8*). However, osteosarcoma has been traditionally regarded as a neoplasm that responds poorly to radiation (*9*), and our current knowledge about the dose–response relationship in [153]Sm-EDTMP therapy is also limited.

Patient-specific, 3-dimensional (3D) treatment planning is a routine procedure in XRT; however, it has been gaining interest in RPT only recently. Osteosarcoma tumors are a heterogeneous mixture of bone and soft tissue, and osseous metastases have increased radiographic density. The uptake of [153]Sm-EDTMP in osteosarcoma tumors and

the radionuclide distribution are also commonly highly non-uniform (10). Hence patient-specific, 3D image–based tumor dosimetry could be helpful in cases of ^{153}Sm-EDTMP therapy to better understand the dose–response relationship.

Even an accurate and detailed absorbed dose calculation is useful only to the extent that it is biologically relevant and easily interpretable. The radiobiologic dosimetry (RD) parameters such as biologically effective dose (BED) and equivalent uniform BED (EUD), which account for difference in absorbed dose rate and nonuniform BED (and absorbed dose) distributions, respectively, are suggested for a better understanding of dose–response relationships (11–13). In this study, we present a tumor dosimetric analysis in high-risk osteosarcoma (defined as a tumor that was recurrent, refractory to conventional therapy, or metastatic, with either >4 tumors, bone metastases, or both) patients who underwent tandem administered activity (dose) of ^{153}Sm-EDTMP.

MATERIALS AND METHODS

Patients and ^{153}Sm-EDTMP Therapy

Thirteen patients with high-grade osteoblastic osteosarcoma participated in a phase I dose-finding study that determined the maximally tolerated dose of ^{153}Sm-EDTMP, with hematopoietic recovery within 6 wk. In a subsequent phase II study designed to study the safety and response of high-risk osteosarcoma to a high dose of ^{153}Sm-EDTMP, 11 of 13 patients who participated in the phase I study were found eligible to receive a second high dose (tandem dose) of ^{153}Sm-EDTMP. The clinical trial details and the treatment plan have been described by Loeb et al. (2,3). Briefly, patients were included in the study if they had a positive ^{99m}Tc-methylene diphosphonate bone scan finding; autologous hematopoietic stem cells were collected before the first treatment with ^{153}Sm-EDTMP (low dose). The low-dose administered activity ranged from 37 to 51.8 MBq/kg (1.0–1.4 mCi/kg). Patients were followed up until hematologic recovery and evaluated for disease response. Approximately 6 wk after the first treatment, a second treatment (high dose) with 222 MBq/kg (6 mCi/kg) of ^{153}Sm-EDTMP was administered. Patients received autologous stem cell infusion 14 d after high-dose ^{153}Sm-EDTMP therapy. The study was approved by the institutional review board of Johns Hopkins University. All patients provided informed consent.

Six of the 13 patients (3 men and 3 women; age range, 12–30 y; mean age, 22 y) underwent ^{153}Sm-EDTMP SPECT/CT for 3D-RD analysis, after either low- or high-dose ^{153}Sm-EDTMP therapy. Table 1 summarizes the demographics and administered activities for the patients who were included in this tumor dosimetric analysis. Five patients underwent SPECT/CT after a low dose of ^{153}Sm-EDTMP and 4 after a high dose; 3 of these patients underwent SPECT/CT after both a low and a high dose of ^{153}Sm-EDTMP. Two patients (patients 3 and 4) did not receive high-dose ^{153}Sm-EDTMP therapy because of their clinical condition. One patient (patient 6) did not undergo SPECT/CT after low-dose ^{153}Sm-EDTMP therapy.

^{153}Sm-EDTMP SPECT/CT and Image Reconstruction

SPECT/CT images over selected tumor regions were obtained at 4 and 48 h or 72 h after ^{153}Sm-EDTMP therapy infusion using a variable-angle dual-head γ-camera, the Millennium VG Hawkeye (GE Healthcare). The SPECT images were acquired using an energy window centered on the 103-keV photopeak with a 20% width. A 128 × 128 matrix, 4.4 mm/pixel, was used, with a 360° rotation (high-resolution, low-energy collimators), 3° step, and 20 s per frame. The CT portion of the study was acquired in helical mode at 2.5 mA and 140 kVp, with a slice step of 1 cm and a slice time of 14 s in a 256 × 256 matrix, 2.2 mm/pixel. Cross-sectional attenuation images (128 × 128 image matrix), in which each pixel represents the attenuation of the imaged tissue, were generated in all cases. γ-camera counting rate saturation was expected at the high ^{153}Sm activity levels seen in the field of view and needed to be considered. Accordingly, the projection images were corrected for γ-camera counting rate saturation, using a method described elsewhere (14). A previously described quantitative SPECT reconstruction method (15) was used for image reconstruction. Attenuation, scatter, and the geometric collimator-detector response function were modeled during the iterative process. The attenuation was modeled using measured CT-based attenuation maps. Scatter compensation was performed using the effective source scatter estimation method with a fast implementation. The geometric-detector response function was computed using an analytic formulation.

Patient-Specific Tumor Dosimetry

We used the 3D-RD software package (12) for patient-specific tumor dosimetric analysis. The 3D-RD software incorporates radiobiologic modeling, using the linear-quadratic model of cell kill, and calculates RD parameters such as BED and EUD to provide a biologic basis for correlations with response. Each step of the 3D-RD calculation procedure is briefly outlined.

Image Registration and Tumor Volume Delineation. The reconstructed SPECT and cross-sectional attenuation CT images (128 × 128 image matrix) were registered to each other across time using a workstation (HERMES Medical Solutions). Because intense ^{153}Sm-EDTMP uptake was observed in all tumors on post–^{153}Sm-EDTMP therapy SPECT images, the coregistered SPECT and attenuation CT images were used for tumor volume delineation. A threshold of 40% of the maximum tumor intensity in the ^{153}Sm-EDTMP SPECT images was used to trace the initial tumor volumes of interest (VOI). With the help of these initial VOIs, the final tumor volumes were delineated manually on the attenuation CT images. Given the area of each region of interest on slice i, A_i, and the slice thickness, θ, the volume of each tumor, V_T, was obtained from:

$$V_T \;=\; \sum_i A_i \times \theta. \qquad \text{Eq. 1}$$

The tumor density at the voxel level, ρ_j, was obtained from the CT image for each voxel, j, using a scanner-specific Hounsfield unit–to–density conversion curve. The tumor mass, M_T, was obtained as the sum of the product of the volume, v_j, and the density, ρ_j, at each voxel in the tumor VOIs:

$$M_T = \sum_j v_j \times \rho_j. \qquad \text{Eq. 2}$$

Monte Carlo Calculations. At each time point, SPECT activity maps and CT-based density maps were input to 3D-RD. Using the electron γ-shower Monte Carlo code (EGS4 DOSXYZnrc), we executed 10 million histories for the electron and photon components of the ^{153}Sm decay spectra with the ^{153}Sm activity distribution as obtained from the SPECT images at each time point. Spectra probability distributions were obtained from the RADTABS program (16).

TABLE 1
Patient Demographics and [153]Sm-EDTMP Treatment

Patient no.	Sex	Age (y)	Mass (kg)	[153]Sm-EDTMP treatment	
				Low administered activity (GBq)	High administered activity (GBq)
1	F	25	85	3.93	17.8
2	F	30	52	2.37	11.5
3*	M	12	52	2.39	—
4*	M	25	101	3.73	—
5	M	21	78	3.57	17.0
6	F	19	75	2.84	16.6

*Patient was not treated with high administered activity.

Tumor-Absorbed Dose. A hybrid trapezoid-exponential model was applied to the tumor VOIs as a whole and to individual voxels making up the dose–rate image at each time point to obtain absorbed dose, D. The hybrid fit consists of a linear fit between the origin and the first time point, another linear fit between the 2 time points, and an exponential tail with the [153]Sm physical decay constant, λ_ϕ, after the second time point.

Tumor BED and EUD. 3D-RD incorporates linear quadratic radiobiologic modeling (*12,17,18*) to calculate BED and EUD.

The formula for the BED is:

$$\text{BED} = D\left(1 + \frac{G(\infty)}{\alpha/\beta} \times D\right), \qquad \text{Eq. 3}$$

where α and β are the respective linear and quadratic radiosensitivity coefficients in the linear quadratic equation, and $G(T)$ is the Lea-Catcheside G factor (*17*). The G factor is a function of another radiobiologic parameter, μ, the DNA repair rate, assumed exponential. The generalized expression of the G factor is:

$$G(T) = \frac{2}{D^2} \times \int_0^T \dot{D}(t)\,dt \int_0^t \dot{D}(w) \times e^{-\mu(t-w)}\,dw, \qquad \text{Eq. 4}$$

where w is an integration variable. For a monoexponential fit to the dose rates, the G factor reduces to:

$$G(\infty) = \frac{\lambda}{\lambda + \mu}. \qquad \text{Eq. 5}$$

On a voxel basis, the kinetics rarely satisfy a monoexponential relationship. In this case, the BED is most easily obtained by numeric integration (*18*) of the general form of $G(T)$. The radiobiologic parameters, $\alpha = 0.28 \text{ Gy}^{-1}$, $\beta = 0.0515 \text{ Gy}^{-2}$, and $\mu = 1.73 \text{ h}^{-1}$, were derived from a human osteosarcoma cell line (*19*) and were used for the calculations of BED and EUD.

The EUD is calculated from the differential BED volume histograms:

$$\text{EUD} = -\frac{1}{\alpha}\ln\left(\sum_{j=1}^{n} \frac{e^{-\alpha \text{BED}_j}}{n}\right), \qquad \text{Eq. 6}$$

where n is the number of voxels, and BED_j are the individual voxel BED values. The EUD is a single uniform value of BED that would produce the same surviving fraction of tumor cells as does the nonuniform distribution.

Tumor Dosimetry Based on Unit-Density Sphere Model

OLINDA/EXM 1.0 was used for the tumor-absorbed dose calculations based on the unit-density sphere model. The OLINDA/EXM unit-density sphere model requires a time-integrated activity coefficient (TIAC) as an input for the absorbed dose calculations. We obtained the TIAC for the tumors from the 3D-RD calculations. First, we obtained the time-integrated activity (cumulated activity) by integrating the activity measured in the tumor VOI over time, using the combination of numeric and analytic integration methods described. The tumor TIAC was then obtained by dividing the time-integrated activity by the administered activity. Because the OLINDA/EXM sphere model gives absorbed dose estimates for discrete masses, we generated dose coefficients (mean absorbed dose per unit administered activity scaled for 1 MBq-h/MBq TIAC) for different masses of [153]Sm. The OLINDA/EXM-generated dose coefficients for [153]Sm for a TIAC of 1 MBq-h/MBq were fitted against the sphere masses using a power-law model of the form:

$$d = am^b, \qquad \text{Eq. 7}$$

where d is the dose coefficient, a and b are fitting parameters, and m is the sphere mass. Using these fitting parameters, we calculated mean tumor-absorbed dose per unit administered activity for each tumor by scaling the output of Equation 7 to the measured TIAC, and the mean tumor-absorbed dose was obtained by multiplying by the administered activity. The density and radionuclide distribution were assumed to be uniform in this method of calculation. To study the impact of tumor density, mass, and nonuniformity in the radionuclide distribution on tumor-absorbed dose, we compared the mean tumor-absorbed dose calculated using the OLINDA/EXM unit-density sphere model with the mean tumor-absorbed dose calculated using the patient-specific 3D-RD method.

We also simulated 15 unit-density spheres of various masses (range, 1–600 g) of uniformly distributed [153]Sm decays using the 3D-RD and generated dose coefficients. These dose coefficients were then compared with the OLINDA/EXM-generated dose coefficients to cross-check 3D-RD and OLINDA/EXM for [153]Sm.

Tumor Sphericity

We used sphericity as a parameter to measure how close the actual tumor shape is to the usual assumption of tumor as a sphere
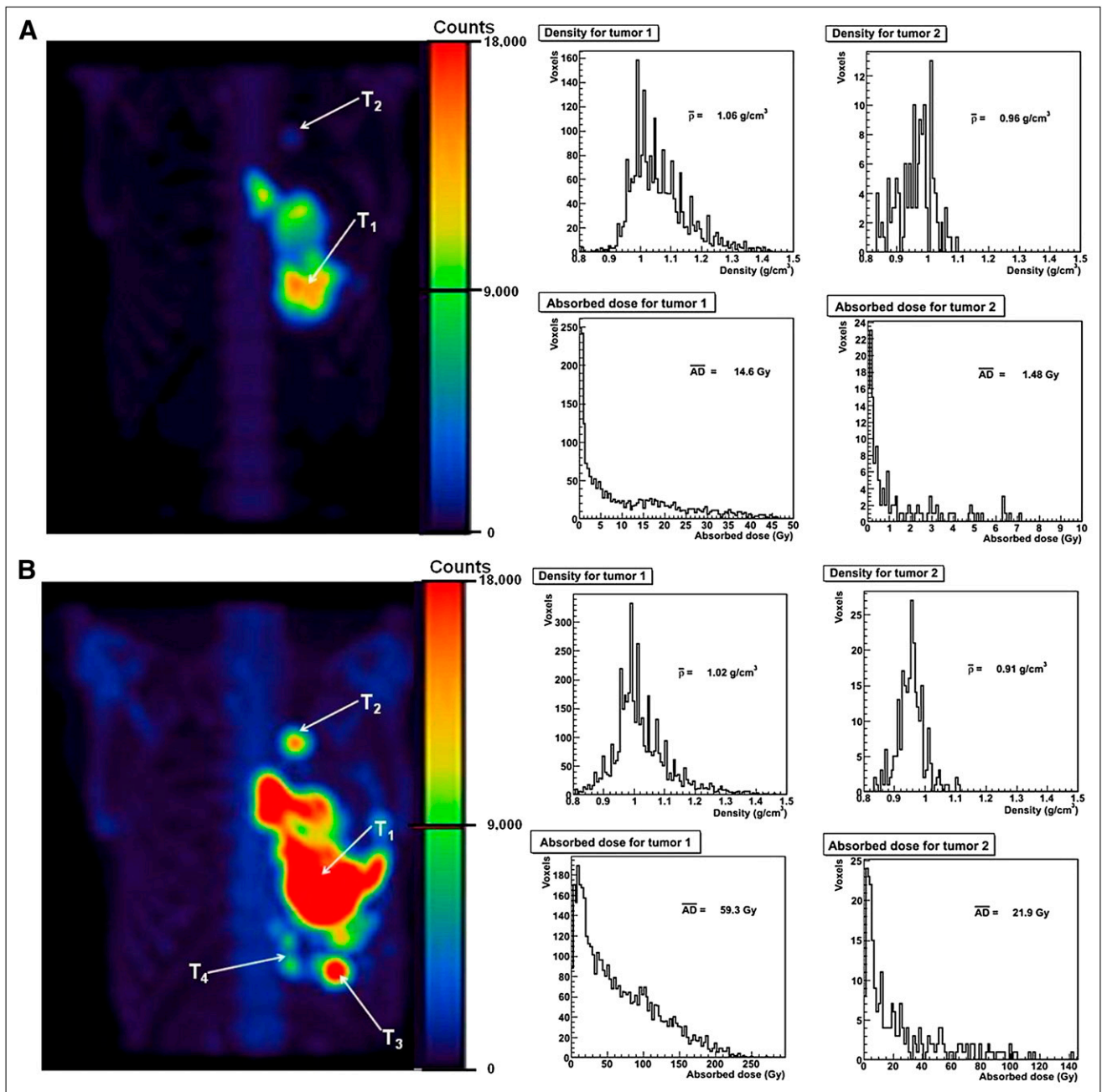
FIGURE 1. Example of 3D-RD analysis. Four hours after low-dose [153]Sm-EDTMP SPECT for patient 2, 2 tumors were identified (T_1 and T_2) for dosimetry analysis (A). Density and dose–volume histograms for tumors are also shown. Four hours after high-dose [153]Sm-EDTMP SPECT for same patient, 2 new tumors (T_3 and T_4) were identified in addition to 2 tumors identified at low-dose therapy (B). Tumor density and dose–volume histograms for 2 old tumors (T_1 and T_2) seen at low-dose therapy are shown for comparison. SPECT images are shown, with same maximum intensity for comparison. AD = absorbed dose.

in dosimetry calculations. Tumor sphericity is defined as the ratio of the surface area of the tumor if it were a sphere (A_S) with the same volume to the surface area of the actual tumor (A_T).

$$\text{Sphericity} = \frac{A_S}{A_T}. \qquad \text{Eq. 8}$$

The tumor surface area (A_T) was obtained by summing the number of voxels at the interface between the tumor and the surrounding tissue and multiplying this number by the surface area of a single-voxel side. Because the voxels are cubic, this method gives a larger surface area than for a smooth curve; the surface area is (at minimum) the sum of the projections of the tumor VOI onto the coordinate axes: front, back, left, right, top, and bottom. Thus, for a voxelized sphere of radius R, the measured surface area will be $6\pi R^2$ rather than $4\pi R^2$. Because our VOIs are voxelized, we normalized our sphericity formula to the voxelized sphere and used $A_S = 6\pi R^2$. This value was confirmed for the

measured surface area of the unit-density spheres used in the OLINDA/EXM comparison. Therefore, the formula for A_S as a function of the measured tumor volume, V_T, becomes:

$$A_S = 3^{5/3}\left(\frac{\pi}{2}\right)^{1/3}V_T^{2/3}. \qquad \text{Eq. 9}$$

Overall Treatment Response

Overall treatment response was evaluated on hematologic recovery from each therapy using either CT or MRI. Radiographic response criteria were as follows: complete response, complete resolution of radiographic evidence of disease; partial response, more than 50% reduction in the sum of the products of perpendicular tumor diameters; minor response, a 25%–50% reduction in the sum of the products of the tumor diameter without the emergence of new lesions and no individual lesion progressing more than 25% in a single dimension; stable disease, no progressive disease; and progressive disease, emergence of new lesions or progression of any lesion by more than 25% in a single dimension.

Individual Tumor Response

MR images were used to measure the change in tumor volume before and after ^{153}Sm-EDTMP low- and high-dose therapy. The percentage reduction in tumor volume ([initial tumor volume – posttherapy tumor volume]/initial tumor volume × 100) was compared against mean tumor-absorbed dose (obtained from whole-tumor VOIs) and EUD (from the voxelized dosimetry calculation and Eq. 6).

Statistical Analysis

Because the overall response accounted for all tumors in each patient, including tumors not evaluated for dosimetry, statistical analysis was confined to the individual tumor dose–response evaluation. Measurements from the multiple tumors in the same patient tend to be positively correlated (cluster). A hierarchical mixed-effects model was used to analyze such clustered data, where within- and between-subject variability was considered by assuming an exchangeable variance–covariance structure. The Kenward–Roger approximation was used to assess the degrees of freedom (20).

RESULTS

A typical 3D-RD tumor dosimetric analysis is shown in Figure 1. ^{153}Sm-EDTMP uptake in tumors was clearly identifiable in both the low- and high-dose posttherapy SPECT images. Heterogeneous tumor densities were observed at the voxel level in all tumors that were studied. In the tumors analyzed, the mean tumor density ranged between 0.8 and 1.3 g-cm^{-3}. The tumor density and absorbed dose volume histograms shown in Figure 1 represent a typical example of the variability observed in all tumors. In the 6-wk interval between the low-dose (Fig. 1A) and high-dose (Fig. 1B) therapy, new tumor growth was also observed in some patients on ^{153}Sm-EDTMP SPECT and was confirmed using CT.

Table 2 summarizes the 3D-RD tumor dosimetric analysis. Six patients (19 tumors) had datasets complete enough for the 3D-RD analysis. The tumor mass ranged between 11 and 633 g. In the 7 tumors (5 patients) that were analyzed at low-dose therapy, the mean and SD of the tumor-absorbed dose, BED, and EUD were 4.5 ± 4.7, 4.6 ± 4.8, and $2.3 \pm$

TABLE 2
Summary of Patient-Specific (3D-RD) Tumor Dosimetry

^{153}Sm-EDTMP treatment	Patient no.	Tumor no.	Tumor mass (g)	Mean absorbed dose (Gy)	Mean biologically effective dose (Gy)	Equivalent uniform dose (Gy)	Percentage tumor volume reduction	Overall treatment response
Low administered activity	1	1	65.2	1.80	1.81	1.22	−56.4	Progressive disease
	2	1	210	14.6	15.1	3.87	−95.2	Progressive disease
		2	10.9	1.48	1.48	0.98	−218	
	3	1	633	2.06	2.06	1.50	−19.5	Progressive disease
	4	1	482	2.85	2.88	2.30	−73.6	Progressive disease
	5	1	43.2	5.45	5.50	3.90	−195	Progressive disease
		2	25.1	3.18	3.16	2.06	−66.7	
High administered activity	1	1	132	4.93	5.06	3.25	NA	Progressive disease
	2	1	379	59.3	87.3	12.3	10.7	Stable disease
		2	20.6	21.9	32.2	6.76	36.4	
		3	18.3	28.4	35.9	8.29	33.8	
		4	21.6	28.6	45.5	5.88	10.5	
	5	1	266	21.6	22.3	9.17	−21.0	Stable disease
		2	36.3	23.8	24.7	8.42	38.2	
	6	1	25.1	2.93	2.96	1.89	NA	Progressive disease
		2	15.0	3.09	3.13	2.30	NA	
		3	23.6	3.13	3.15	2.16	NA	
		4	18.0	5.45	5.62	2.32	NA	
		5	41.4	3.33	3.35	1.95	NA	

NA = not available.

1.2 Gy, respectively. In the 12 tumors (4 patients) that were analyzed at high-dose therapy, the mean and SD of tumor-absorbed dose, BED, and EUD were 17.2 ± 17.0, 22.6 ± 25.4, and 5.4 ± 3.6 Gy, respectively. The 5-fold increase in administered activity from low- to high-dose therapy resulted in an approximately 4-fold (3.8) increase in mean tumor-absorbed dose averaged over the treated patients. However, the equivalent uniform dose on average increased only about 2-fold (2.4). In 5 tumors (3 patients) that were treated at both low- and high-dose therapy, the average ratio of mean tumor-absorbed dose in the same tumors that were treated at both low and high dose was 6.6 and ranged from 2.7 to 14.8. In 2 patients (1 and 6), the percentage reduction in tumor volume could not be measured after high-dose therapy, because the patients had disease progression and did not return for follow-up radiographic evaluation.

Figures 2A and 2B show the tumor mass and mean density dependence of mean tumor-absorbed dose. A large variation was observed in the mean tumor-absorbed dose across individual tumors in the 6 patients studied. No relationship between mean tumor-absorbed dose and tumor mass or tumor density could be discerned. Likewise, Figures 2C and 2D show no corresponding relationship for EUD.

Figure 3A shows the curve fit for the OLINDA/EXM dose coefficients for the unit-density spheres of various masses for ^{153}Sm. The fit parameters were $a = 149.9$ and $b = -0.9886$. Figure 3B shows the percentage difference in dose coefficients for individual sphere mass between 3D-RD and OLINDA/EXM (percentage difference, mean $\pm$ SD, $-1.3\% \pm 0.01\%$; range, -0.4% to -3.9%). The percentage difference in the mean tumor-absorbed dose between the patient-specific 3D-RD and the OLINDA/EXM unit-density sphere model ranged between -0.5% and 4%. Figures 4A–4C compare 3D-RD–calculated patient tumor-absorbed doses (obtained from the whole-tumor VOI) with OLINDA-derived estimates. The results show that 3D-RD values were greater by no more than 4%, compared with the
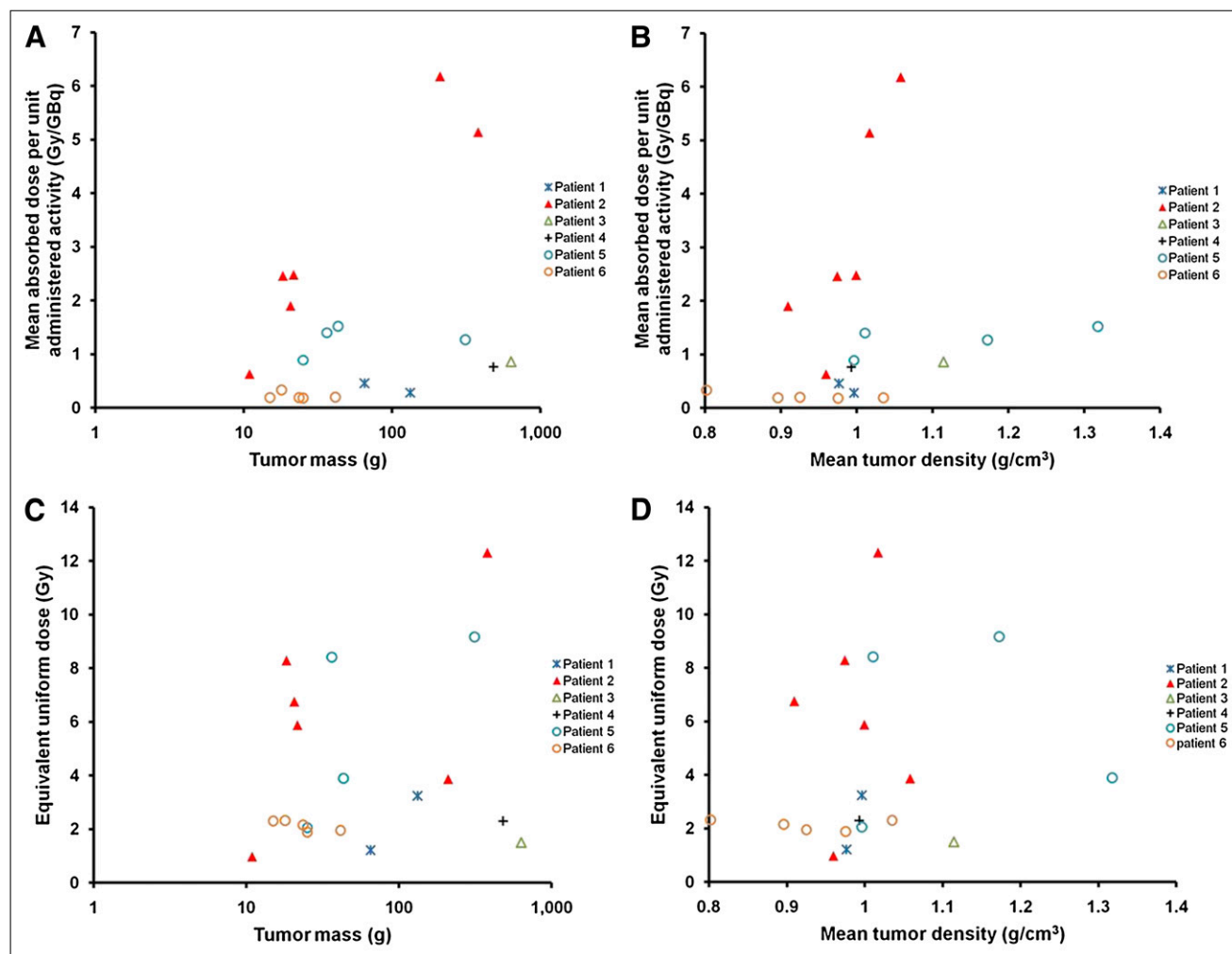

FIGURE 2. Patient-specific 3D-RD tumor dosimetry analyses. Plots of tumor mass and mean tumor density against mean tumor-absorbed dose per unit administered activity (A and B, respectively) and tumor mass and mean tumor density dependence of equivalent uniform dose (C and D, respectively) are shown. Tumor mass is plotted in logarithmic scale in A and C.
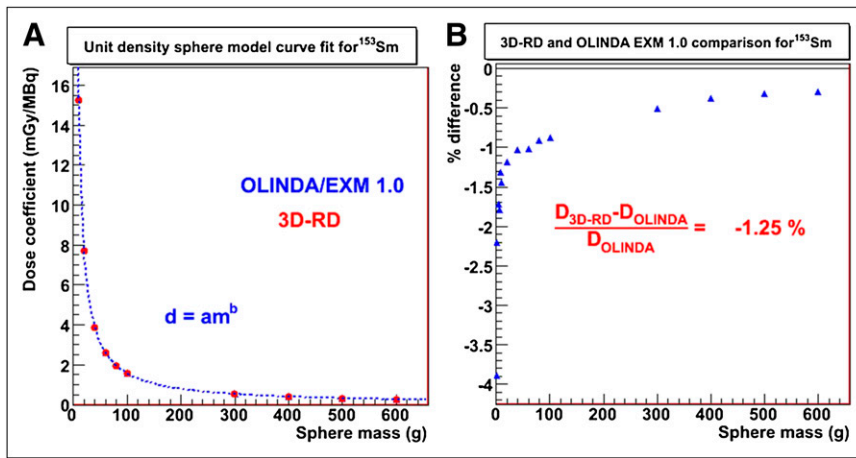
FIGURE 3. Mean absorbed dose calculation based on unit-density sphere model. (A) Power-law fit (dotted line) to OLINDA/EXM dose coefficients against ^{153}Sm-filled homogeneous unit-density spheres of various masses (1–600 g) is demonstrated. 3D-RD–generated dose coefficients are shown as solid point for each sphere on curve fit for comparison. (B) Percentage difference between 3D-RD and OLINDA/EXM for each sphere is given.

OLINDA estimates. This is because the 3D-RD calculation accounts for dose contributions from other source volumes in the body. The effect of tumor mass, density, and sphericity is examined to see if any trends may be discerned in the already small differences found. Figure 4A shows that the percentage difference in mean tumor-absorbed dose was (marginally) larger for tumor masses less than 60 g. To some extent, this difference depends on the tumor location relative to normal organ activity distribution and on the cross-organ contribution to the mean tumor-absorbed dose. In general, however, the mean tumor-absorbed dose to smaller tumors was influenced by external dose contributions to a greater extent than the mean absorbed dose to larger tumors. There was no clear trend observed for the mean tumor-absorbed dose comparison with mean tumor density. The sphericity of the tumors ranged between 0.63 and 0.99. Figure 4C shows the percentage difference in mean tumor-absorbed dose between 3D-RD and OLINDA/EXM as a function of sphericity of the tumors. Smaller tumors formed a cluster on the sphericity plot around 1.0 (equivalent to a sphere). Larger tumors formed a cluster around 0.6 (equivalent to a tetrahedron), exhibiting nonspheric shape.

Radiographic response of disease was evaluated after recovery from the first, low-dose therapy and again after recovery from the higher-dose therapy. All 6 patients experienced disease progression after low-dose therapy. Two patients (2 and 5) had stable disease after the high-dose treatment. As noted in a previous publication (2), the median time to progression was 79 d for the entire cohort of patients. Two patients achieved prolonged survival (990 and 1,432 d), despite eventual disease progression. Figure 5 shows the mean tumor-absorbed dose and EUD for individual tumors, categorized by overall patient response. The plot indicates that the tumors identified in patients who had disease stabilization had received at least a 21-Gy mean absorbed dose and correspondingly a tumor EUD of 6 Gy. Because the absorbed dose was not calculated for all tumors used in the overall response evaluation, the significance of the observed 21-Gy mean tumor-absorbed dose threshold for progressive disease versus stable disease and corre-

sponding 6-Gy threshold for EUD depends on the degree to which the collection of individual calculated mean tumor-absorbed doses reflects the mean absorbed dose to all of the tumors in each patient. As shown in Figure 2, this depends on the patient and on the dosimetry parameter. For example, the average absorbed dose per administered activity for any one of the tumors in patients 5, 6, and possibly 1 is likely to reflect the average absorbed dose to all tumors, whereas this is not the case for patient 2. Because the EUD also accounts for spatial nonuniformity, the EUD for any 1 patient tumor is less likely to reflect the EUD for the collection of patient tumors, and we see approximately the same EUD in each of the 5 analyzed tumors for patient 6.

Individual tumor response versus dose data is shown in Figure 6. Tumors grew when the mean absorbed dose or EUD was below 21 or 6 Gy, respectively. Statistical analysis of these data suggests that both mean tumor-absorbed dose and EUD are positively related to percent tumor volume reduction ($P = 0.031$ and 0.023, respectively).

DISCUSSION

Osteosarcoma patients have poor prognosis if adequate surgical resection is not possible. In chemorefractory and radiotherapy-ineligible osteosarcoma patients, ^{153}Sm-EDTMP therapy offers viable treatment options where none exists. It is a common practice in other tumor types to administer ^{153}Sm-EDTMP on the basis of dose-escalation studies, delivered on the basis of an administered activity per kilogram of body mass or per square meter body surface area. Such an approach is inherently not patient-specific because the localization and clearance characteristics of the agent in individual patients are not considered. Prior dosimetry studies on ^{153}Sm-EDTMP therapy have predominantly used planar/SPECT images for activity quantification, and the tumor dosimetry was based on MIRD S values (21–23). The heterogeneous mixture of bone and soft tissue in osteosarcoma tumors results in nonuniform uptake of ^{153}Sm-EDTMP, and the spatial density might influence the tumor-absorbed dose distribution. Tumor dosimetric analysis looking into the factors influencing the absorbed
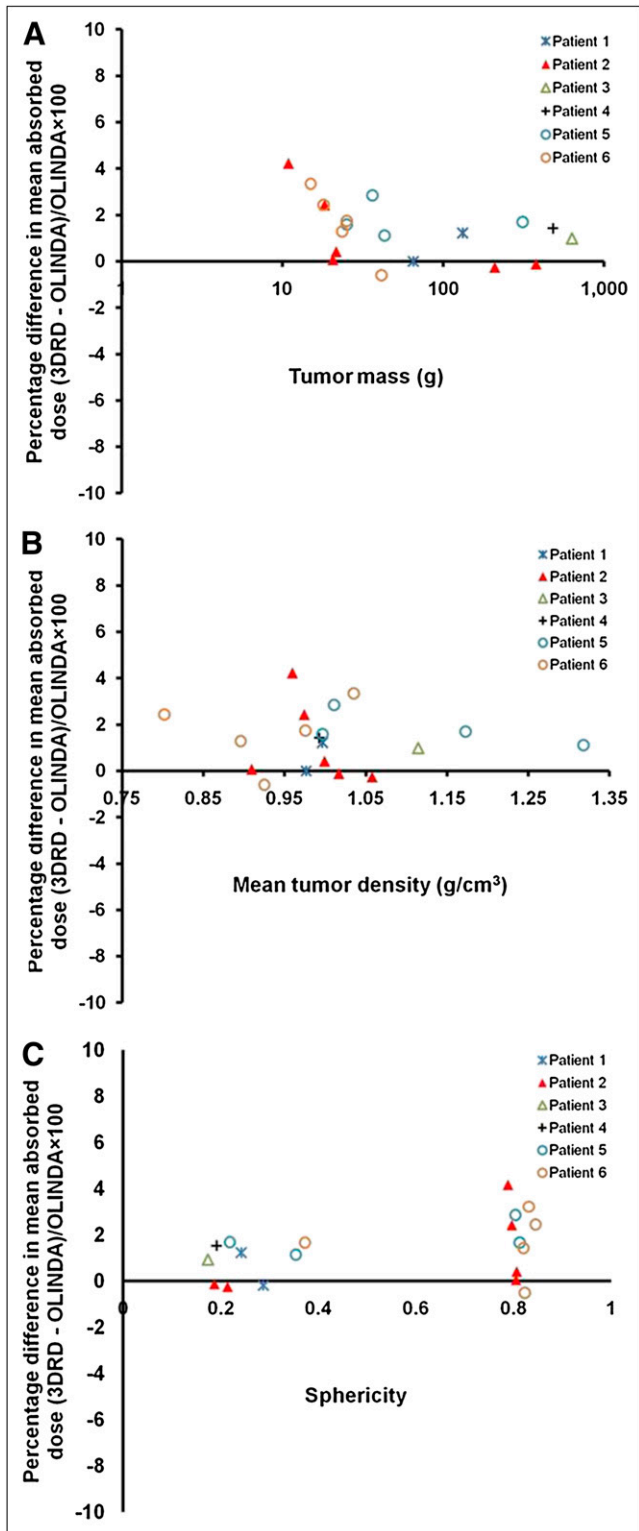
FIGURE 4. Comparison of percentage difference in mean absorbed dose estimates between 3D-RD and OLINDA/EXM unit-density sphere model as function of individual patient tumor mass (A), density (B), and sphericity (C). Tumor mass is in logarithmic scale in A.
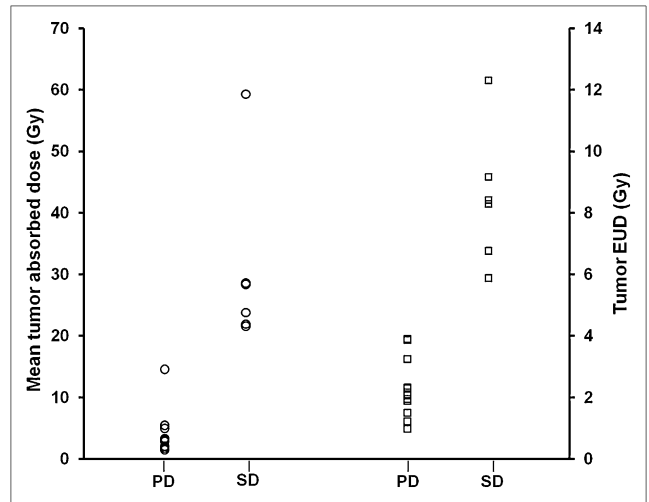

FIGURE 5. Mean tumor-absorbed dose (left *y*-axis) and EUD (right *y*-axis) for individual tumors, plotted against overall radiographic response criteria. PD = progressive disease; SD = stable disease.

dose distributions for individual patients has not been reported for ^{153}Sm-EDTMP therapy of osteosarcoma. Radiobiologic parameters such as BED and EUD have the potential to correlate with the clinical response (*11,13,24*). In this study, we explored the applicability of patient-specific 3D-RD analysis for ^{153}Sm-EDTMP therapy of osteosarcoma.
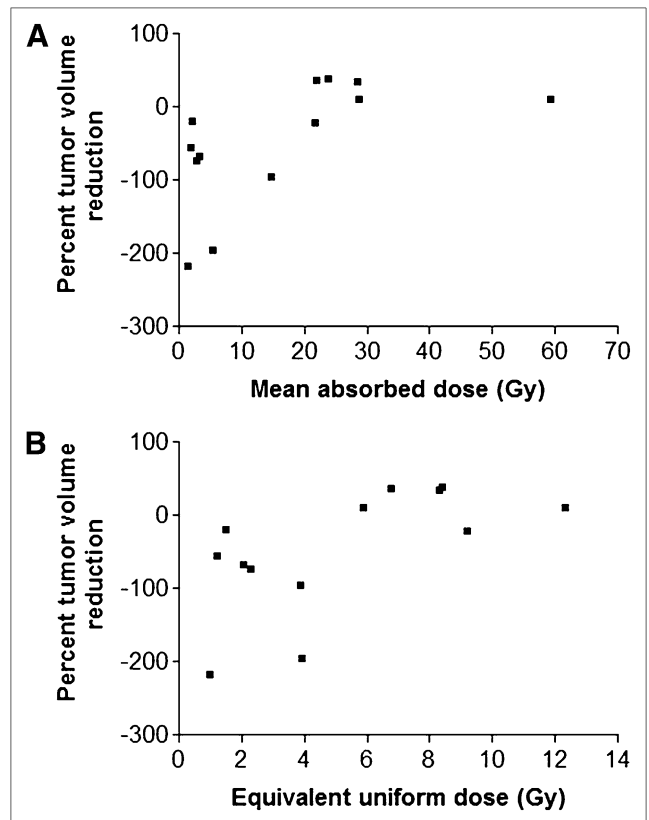

FIGURE 6. Plot of percentage volume reduction against mean tumor-absorbed dose (A) or EUD (B).

Tumor density and absorbed dose volume histograms showed a substantial heterogeneity in these 2 parameters for individual tumors. The mean absorbed dose to individual tumors was not related to tumor mass or tumor density. In general, greater administered activity led to greater mean tumor-absorbed dose, and a 5-fold increase in the administered activity led to a 4-fold increase in the tumor mean absorbed dose averaged over the high- versus low-dose–treated patients. This less than 1-to-1 correspondence in mean tumor-absorbed dose versus administered activity from low- to high-dose therapy could be attributed to known saturation of ^{153}Sm-EDTMP at high administered activities (25,26). 3D-RD–derived dose coefficients for unit-density spheres of different sizes matched corresponding values obtained using OLINDA/EXM. 3D-RD–derived mean tumor-absorbed doses for individual patient tumors were within 5% of values obtained using the OLINDA/EXM unit-density sphere module. Within this 5%, 3D-RD values tended to be greater than OLINDA values. These results suggest that density and dose variations within the tumors analyzed could be neglected in calculating the mean tumor-absorbed dose. The tendency toward greater 3D-RD doses reflects contributions to the tumor-absorbed dose from extratumoral activity, which is consistent with the results showing a proportionately larger external absorbed dose contribution for the smaller tumors.

One of the limitations of the present study is that we had only 2 time point images for time-integrated activity and absorbed dose estimations. Also in SPECT/CT–based dosimetry, uncertainties at the voxel level are important. In particular, SPECT attenuation, CT image resolution, and partial-volume effects might influence the accuracy of voxel-based activity estimation and tissue-density estimations.

In the limited number of patients and tumors that were analyzed in this study, tumor-absorbed dose and EUD thresholds could be identified that separated progressive versus stable overall disease response and tumor growth versus shrinkage. A statistically significant dose–versus–tumor volume shrinkage correlation was obtained for both mean absorbed dose and EUD. Reflecting the highly nonuniform absorbed dose distribution within tumors, the tumor EUD was approximately 2- and 3-fold lower than the mean absorbed dose for low- and high-dose therapy, respectively. In all cases, the tumor volume shrinkage was transient, and tumor growth and disease progression and eventual death were observed in all treated patients, suggesting that substantially higher EUD is required for long-term tumor control.

A recent report summarizing XRT (primarily proton beam) experience in osteosarcoma therapy suggests that an absorbed dose of 69 Gy is required to achieve long-term (>3-y) tumor control in this patient population (27). Because XRT is uniformly delivered, this suggests that EUD values of this order are required to achieve a similar level of tumor control using ^{153}Sm-EDTMP radiopharmaceutical therapy. An approach that combines XRT with RPT has recently been described (28). Combination of XRT with ^{153}Sm-EDTMP treatment presents a possible advantage by providing a localized high absorbed dose to the visible tumors while enabling treatment of occult disease.

CONCLUSION

In this study, we showed the applicability of patient-specific tumor dosimetry in studying the nonuniform absorbed dose distribution of osteoid-forming tumors. The variations in tumor density, mass, and shape seen in these tumors did not affect the mean tumor-absorbed dose estimation significantly. A dose–response relationship was observed for transient tumor volume shrinkage.

DISCLOSURE STATEMENT

ACKNOWLEDGMENTS

REFERENCES

1. PosthumaDeBoer J, Witlox MA, Kaspers GJ, van Royen BJ. Molecular alterations as target for therapy in metastatic osteosarcoma: a review of literature. *Clin Exp Metastasis.* 2011;28:493–503.
2. Loeb DM, Hobbs RF, Okoli A, et al. Tandem dosing of samarium-153 ethylenediamine tetramethylene phosphoric acid with stem cell support for patients with high-risk osteosarcoma. *Cancer.* 2010;116:5470–5478.
3. Loeb DM, Garrett-Mayer E, Hobbs RF, et al. Dose-finding study of ^{153}Sm-EDTMP in patients with poor-prognosis osteosarcoma. *Cancer.* 2009;115:2514–2522.
4. Coronado M, Redondo A, Coya J, et al. Clinical role of Sm-153 EDTMP in the treatment of painful bone metastatic disease. *Clin Nucl Med.* 2006;31:605–610.
5. Sartor O. Overview of samarium sm 153 lexidronam in the treatment of painful metastatic bone disease. *Rev Urol.* 2004;6:S3–S12.
6. Welsh JS, Thurman SA, Borzillary S, Schwartz CL, Howard SP. Sm-153 EDTMP for recurrent metastatic osteosarcoma. *Clin Adv Hematol Oncol.* 2003;1:181–183.
7. Serafini AN. Samarium Sm-153 lexidronam for the palliation of bone pain associated with metastases. *Cancer.* 2000;88:2934–2939.
8. Franzius C, Bielack S, Sciuk J, Vollet B, Jurgens H, Schober O. High-activity samarium-153-EDTMP therapy in unresectable osteosarcoma. *Nuklearmedizin.* 1999;38:337–340.
9. Ogawa Y, Takahashi T, Kobayashi T, et al. Mechanism of apoptotic resistance of human osteosarcoma cell line, HS-Os-1, against irradiation. *Int J Mol Med.* 2003;12:453–458.
10. Singh A, Holmes RA, Farhangi M, et al. Human pharmacokinetics of samarium-153 EDTMP in metastatic cancer. *J Nucl Med.* 1989;30:1814–1818.
11. O'Donoghue JA. Implications of nonuniform tumor doses for radioimmunotherapy. *J Nucl Med.* 1999;40:1337–1341.
12. Prideaux AR, Song H, Hobbs RF, et al. Three-dimensional radiobiologic dosimetry: application of radiobiologic modeling to patient-specific 3-dimensional imaging-based internal dosimetry. *J Nucl Med.* 2007;48:1008–1016.
13. Dewaraja YK, Schipper MJ, Roberson PL, et al. ^{131}I-tositumomab radioimmunotherapy: initial tumor dose-response results using 3-dimensional dosimetry including radiobiologic modeling. *J Nucl Med.* 2010;51:1155–1162.

14. Hobbs RF, Baechler S, Senthamizhchelvan S, et al. A gamma camera count rate saturation correction method for whole-body planar imaging. *Phys Med Biol.* 2010;55:817–831.

15. He B, Du Y, Song X, Segars WP, Frey EC. A Monte Carlo and physical phantom evaluation of quantitative In-111 SPECT. *Phys Med Biol.* 2005;50:4169–4185.

16. Eckerman KF, Endo A. *MIRD: Radionuclide Data and Decay Schemes.* 1st ed. Reston, VA: Society of Nuclear Medicine; 2008.

17. Fowler JF. The linear-quadratic formula and progress in fractionated radiotherapy. *Br J Radiol.* 1989;62:679–694.

18. Hobbs RF, Sgouros G. Calculation of the biological effective dose for piecewise defined dose-rate fits. *Med Phys.* 2009;36:904–907.

19. Brenner DJ, Hall EJ. Conditions for the equivalence of continuous to pulsed low dose rate brachytherapy. *Int J Radiat Oncol Biol Phys.* 1991;20:181–190.

20. Kenward MG, Roger JH. Small sample inference for fixed effects from restricted maximum likelihood. *Biometrics.* 1997;53:983–997.

21. Turner JH, Claringbold PG, Hetherington EL, Sorby P, Martindale AA. A phase I study of samarium-153 ethylenediaminetetramethylene phosphonate therapy for disseminated skeletal metastases. *J Clin Oncol.* 1989;7:1926–1931.

22. Eary JF, Collins C, Stabin M, et al. Samarium-153-EDTMP biodistribution and dosimetry estimation. *J Nucl Med.* 1993;34:1031–1036.

23. Bayouth JE, Macey DJ, Kasi LP, Fossella FV. Dosimetry and toxicity of samarium-153-EDTMP administered for bone pain due to skeletal metastases. *J Nucl Med.* 1994;35:63–69.

24. Sgouros G, Frey E, Wahl R, He B, Prideaux A, Hobbs R. Three-dimensional imaging-based radiobiological dosimetry. *Semin Nucl Med.* 2008;38:321–334.

25. Bartlett M, Webb M, Durrant S, Morton J, Allison R, Macfarlane D. Dosimetry and toxicity of Quadramet for bone marrow ablation in multiple myeloma and other haematological malignancies. *Eur J Nucl Med Mol Imaging.* 2002;29:1470–1477.

26. Erwin W, Mikell J, Ueno N. Predictive value of a pre-therapy tracer study skeletal retention estimate in high-dose Sm-153 EDTMP radiotherapy of skeletal metastatic breast cancer [abstract]. *J Nucl Med.* 2010;51:204P.

27. Ciernik IF, Niemierko A, Harmon DC, et al. Proton-based radiotherapy for unresectable or incompletely resected osteosarcoma. *Cancer.* 2011;117:4522–4530.

28. Hobbs RF, McNutt T, Baechler S, et al. A treatment planning method for sequentially combining radiopharmaceutical therapy and external radiation therapy. *Int J Radiat Oncol Biol Phys.* 2011;80:1256–1262.